

Effects of non-uniform heat transfer in a tempering process on glass quality

Antti Mikkonen¹, Reijo Karvinen¹

Antti Aronen², Mikko Rantala³

¹ Tampere University of Technology, Finland

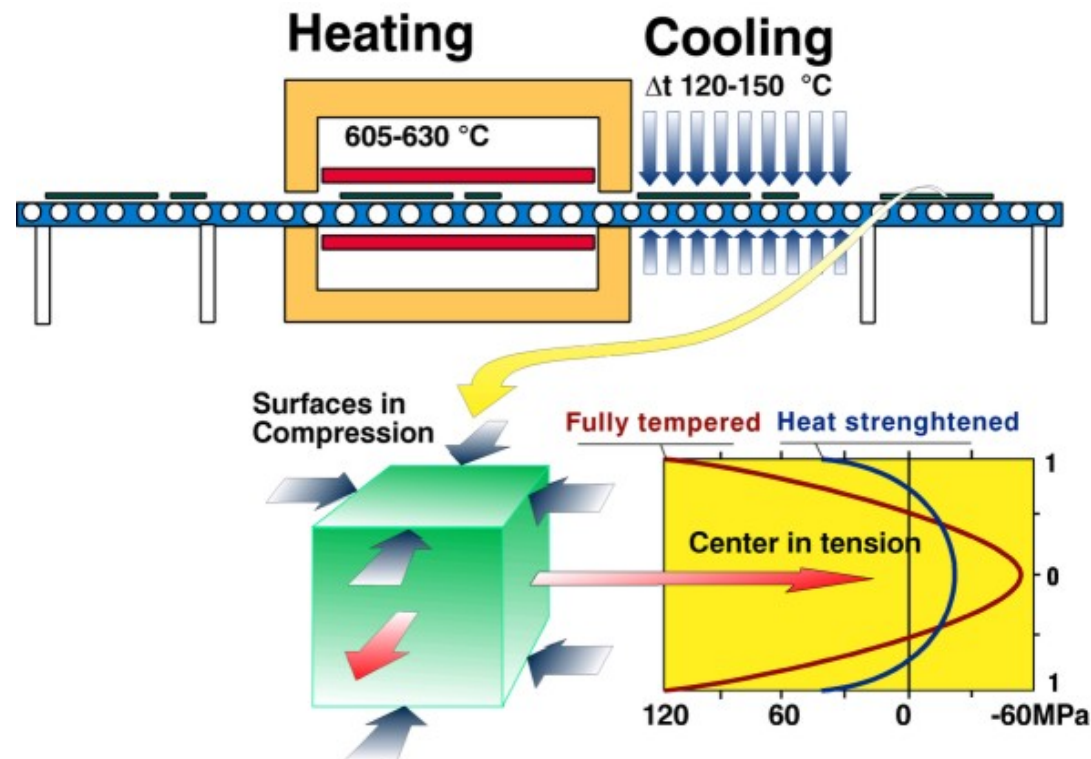
² The University of Sydney, School of Physics, Australia

³ Glaston Finland Oy, Finland

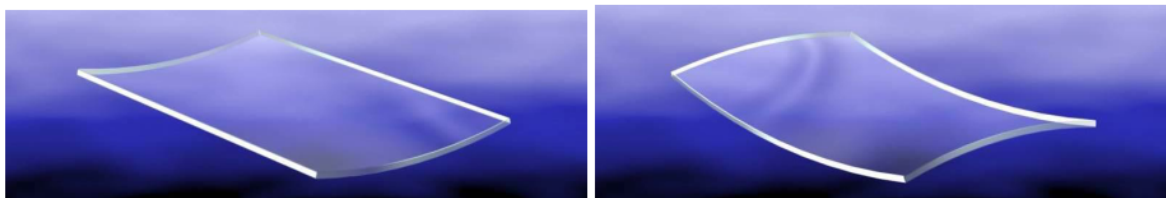
Content

- Requirements in heating and cooling
- Typical quality defects
 - Large scale defects
 - Anisotropy
- Modeling of heat transfer and residual stresses
- Convection heat transfer of impinging jets
- Residual stresses
- Conclusions

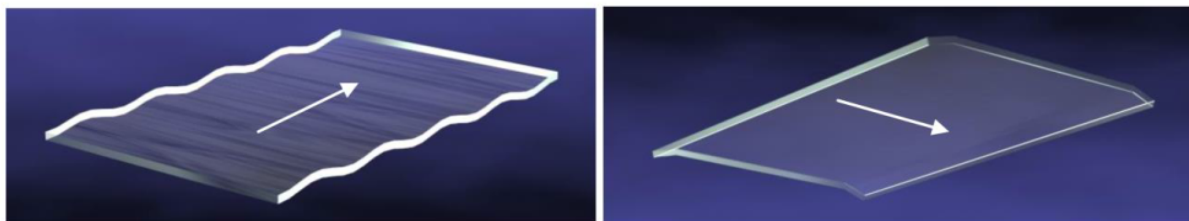
Principle of mechanical tempering



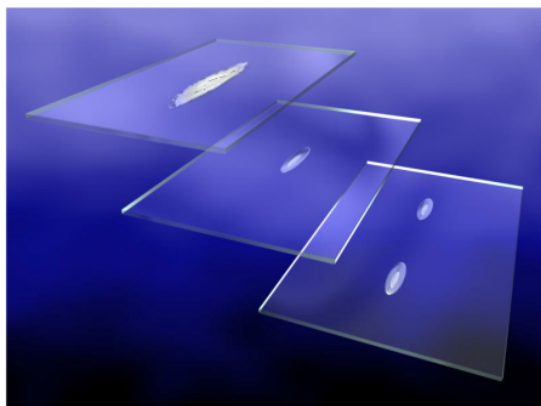
Large scale defects



Convex and saddle-shaped tempered glass



Roller waves and edge lifts



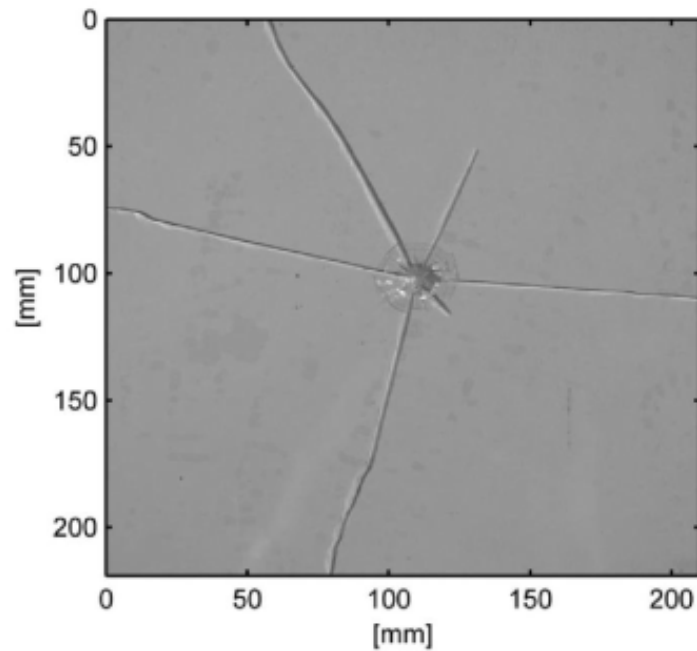
White haze and local optical failures on glass surface

Broken annealed glasses



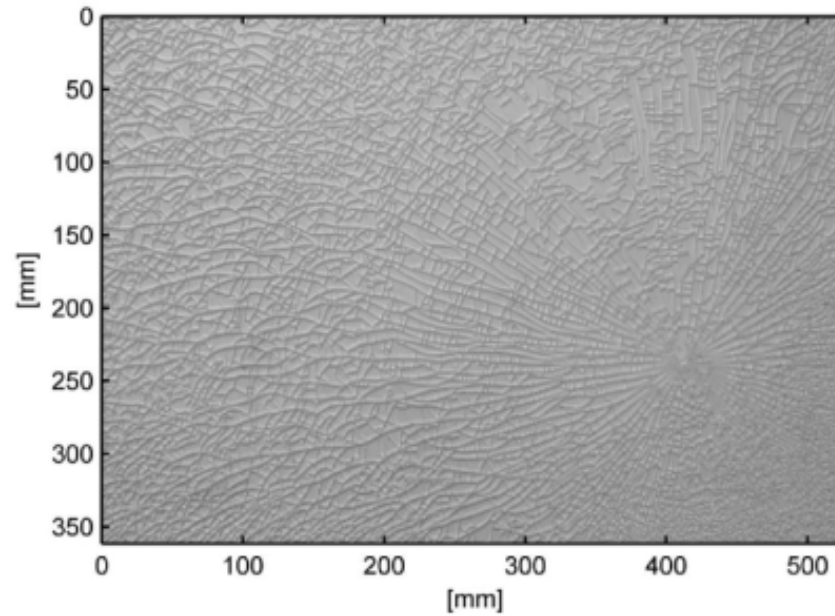
$$\sigma_{zz} = \sigma_{yy} = \frac{\alpha E}{1-\nu} \left(-T + \frac{1}{L} \int_0^L T dx + \frac{3x}{2(L/2)^3} \int_0^L T x dx \right)$$

Tempered Glass



Annealed Glass Breaking Pattern

Aronen 2012 [1]



Tempered Glass Breaking Pattern

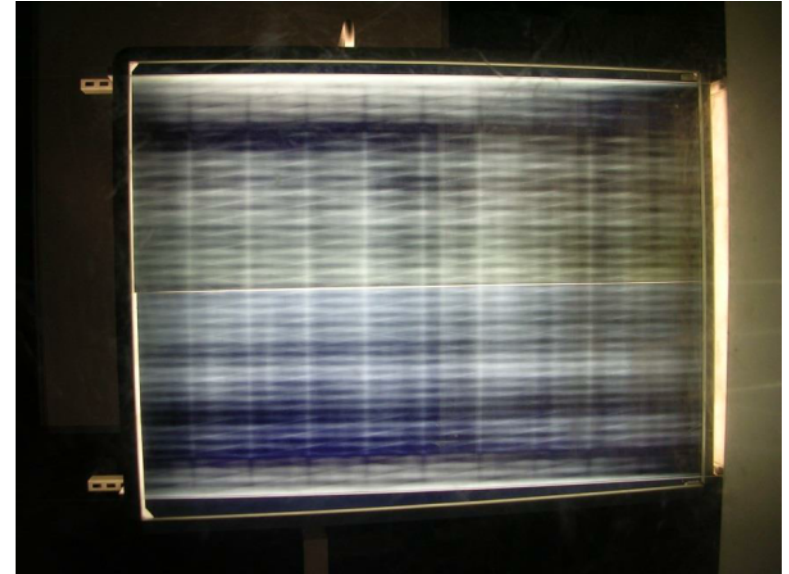
Aronen 2012 [1]

Visual defects

- Uneven heat transfer causes visual defects known as anisotropy
- In our presentation the connection between anisotropy and residual stresses is shown

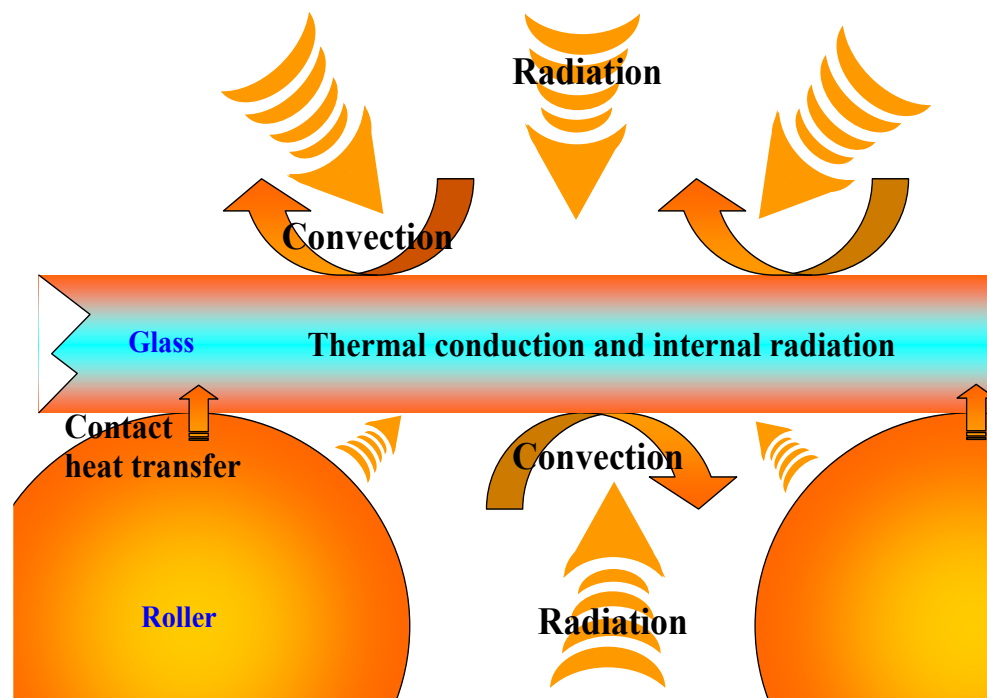


Longitudinal patterns (Henriksen & Leosson 2009).



Typical stress pattern of flat tempered glass seen through polarized filters

Heating of glass



Heating glass in tempering furnace

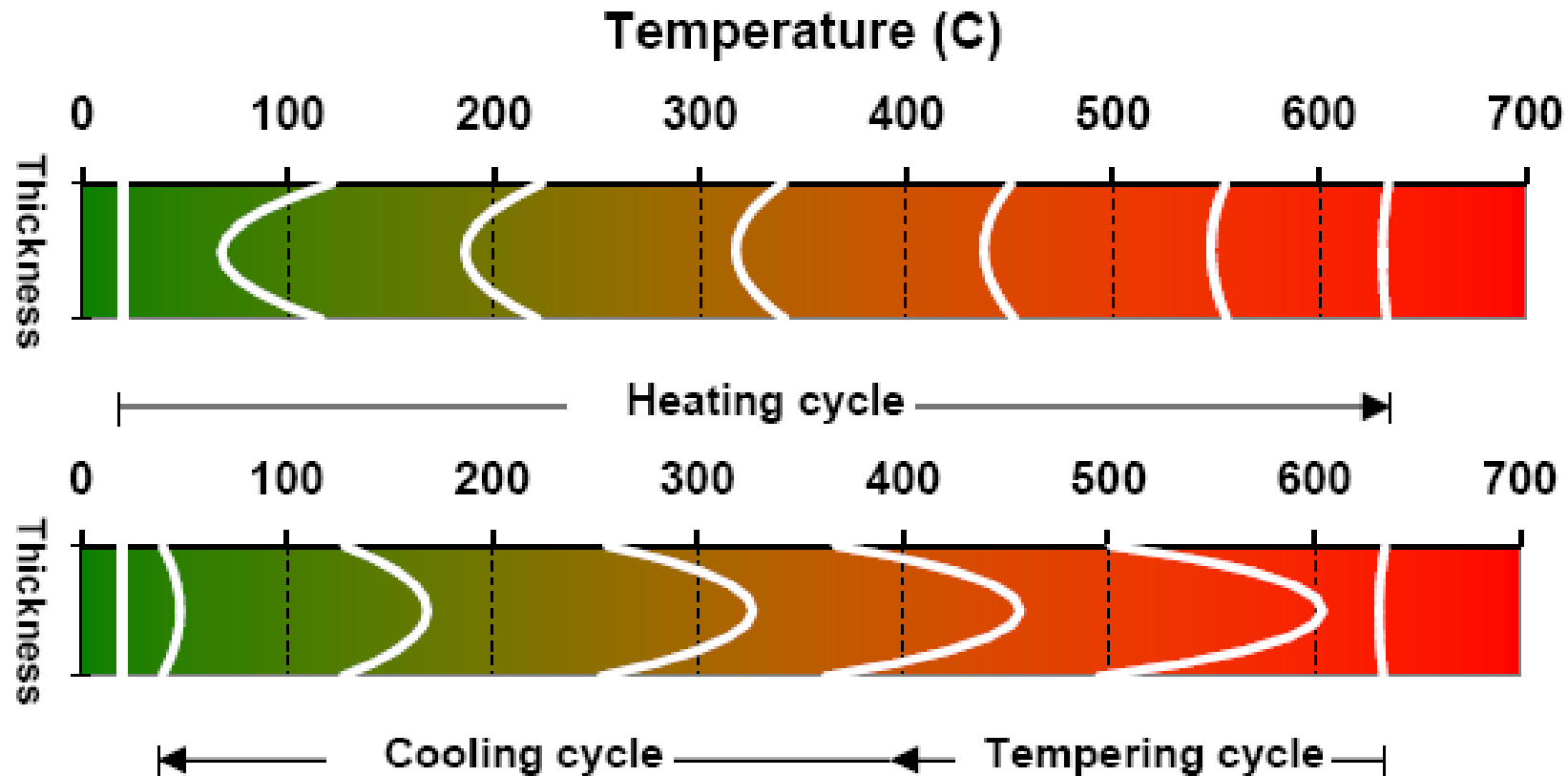
$$\rho c_{pg} \frac{\partial T}{\partial t} = \frac{\partial}{\partial x} \left(k \frac{\partial T}{\partial x} \right) + S$$

$$T(x,0) = T_s$$

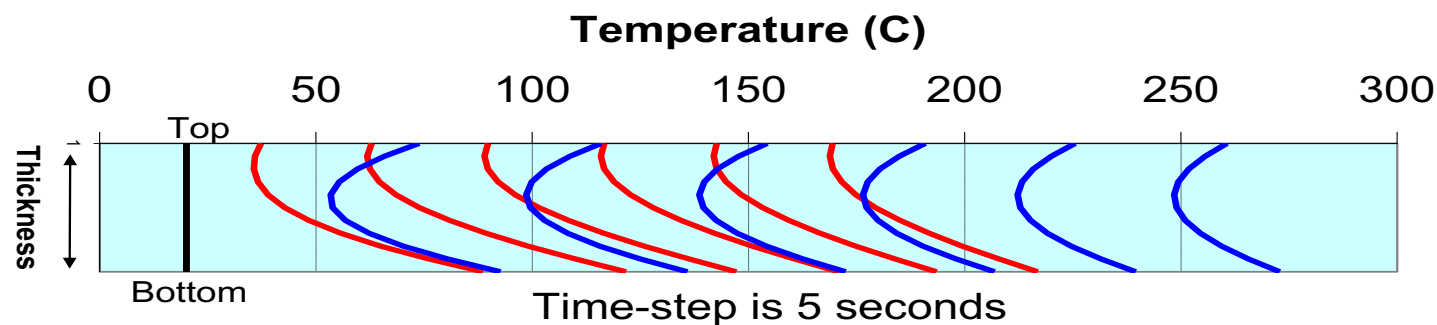
$$k \frac{\partial T(l,t)}{\partial x} = q_{r,u} + q_{c,u}$$

$$-k \frac{\partial T(0,t)}{\partial x} = q_{r,d} + q_{c,d} + q_{con,d}$$

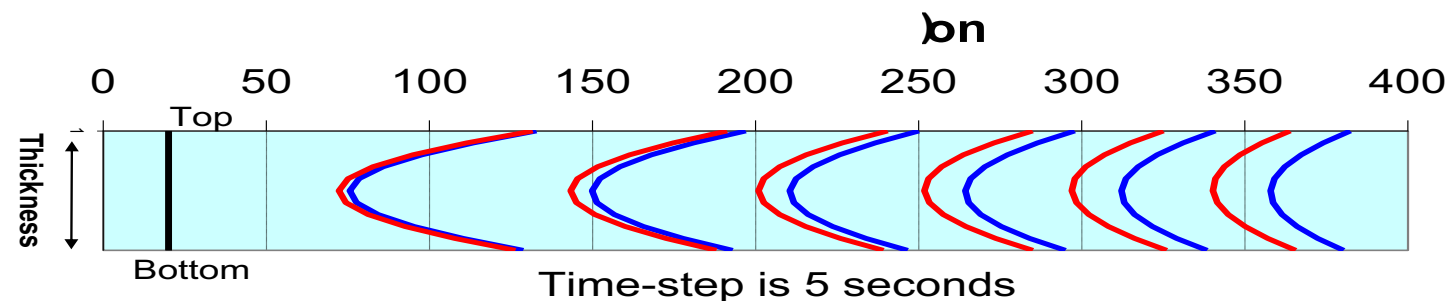
Temperature distributions during heating and cooling



No forced
convection



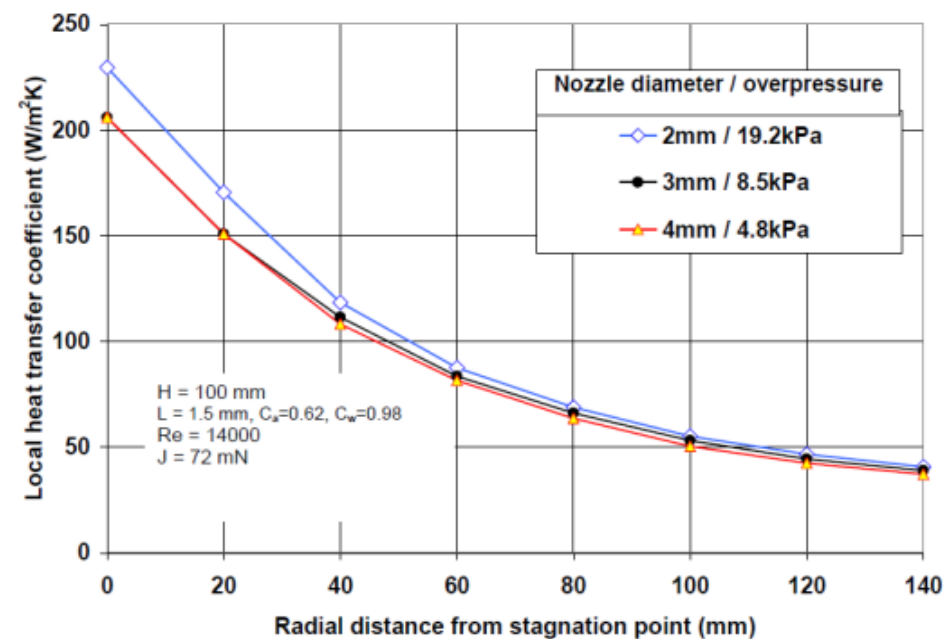
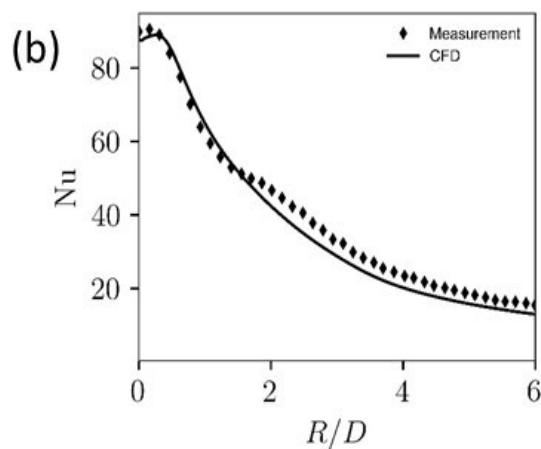
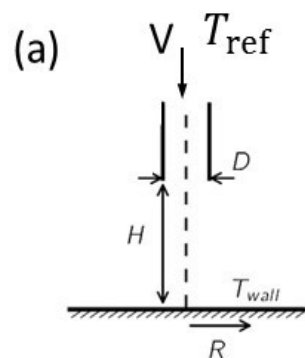
With forced
convection



Clear glass 4mm

Low-e glass 4mm

Heat transfer coefficients of different jets



Black body radiation

$$e_b(\lambda, T) = \frac{C_1}{\lambda^5 (e^{C_2/\lambda T} - 1)} \quad (7.6)$$

This is known as *Planck's* spectral distribution of the blackbody emissive power. In Eq. (7.6) $C_1 = 2\pi^5 k^4 / 15 h^3 c^2 = 3.7419 \times 10^{-16} \text{ Wm}^2$ and $C_2 = hc_0/k = 14,388 \text{ } \mu\text{mK}$, where k is *Boltzmann's* constant and h is *Planck's* constant. Eq. (7.6) is plotted for three surface temperatures in Figure 7.2.

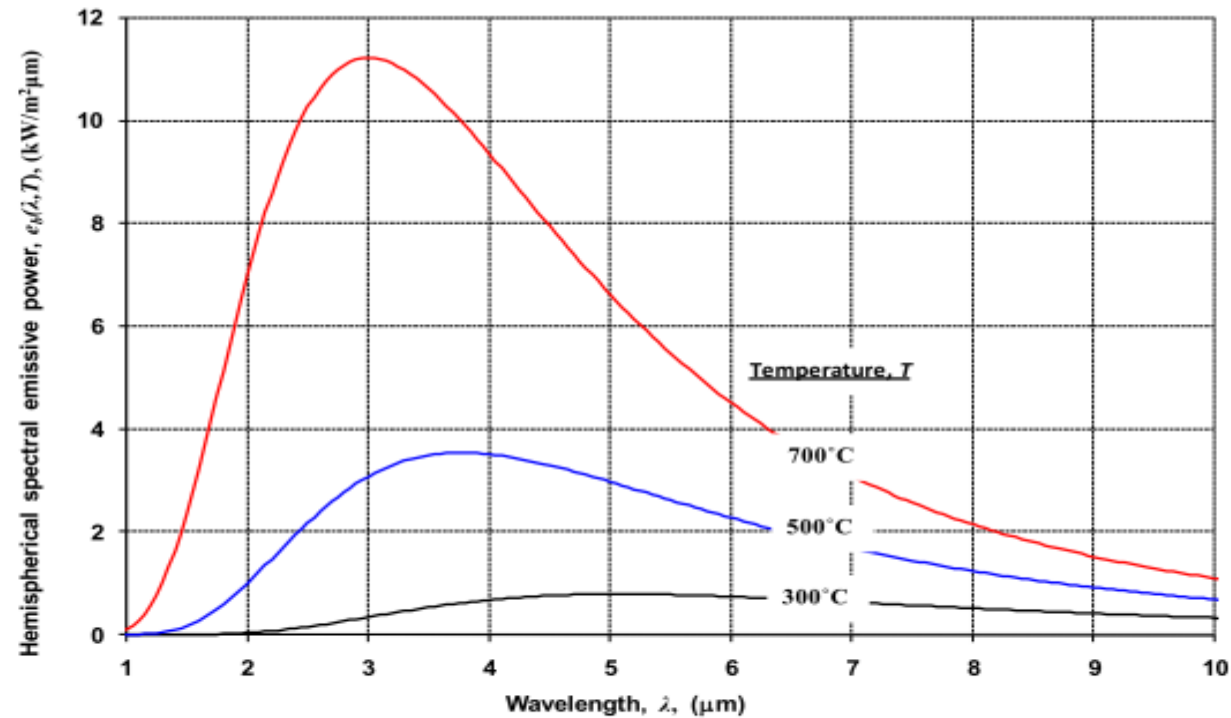
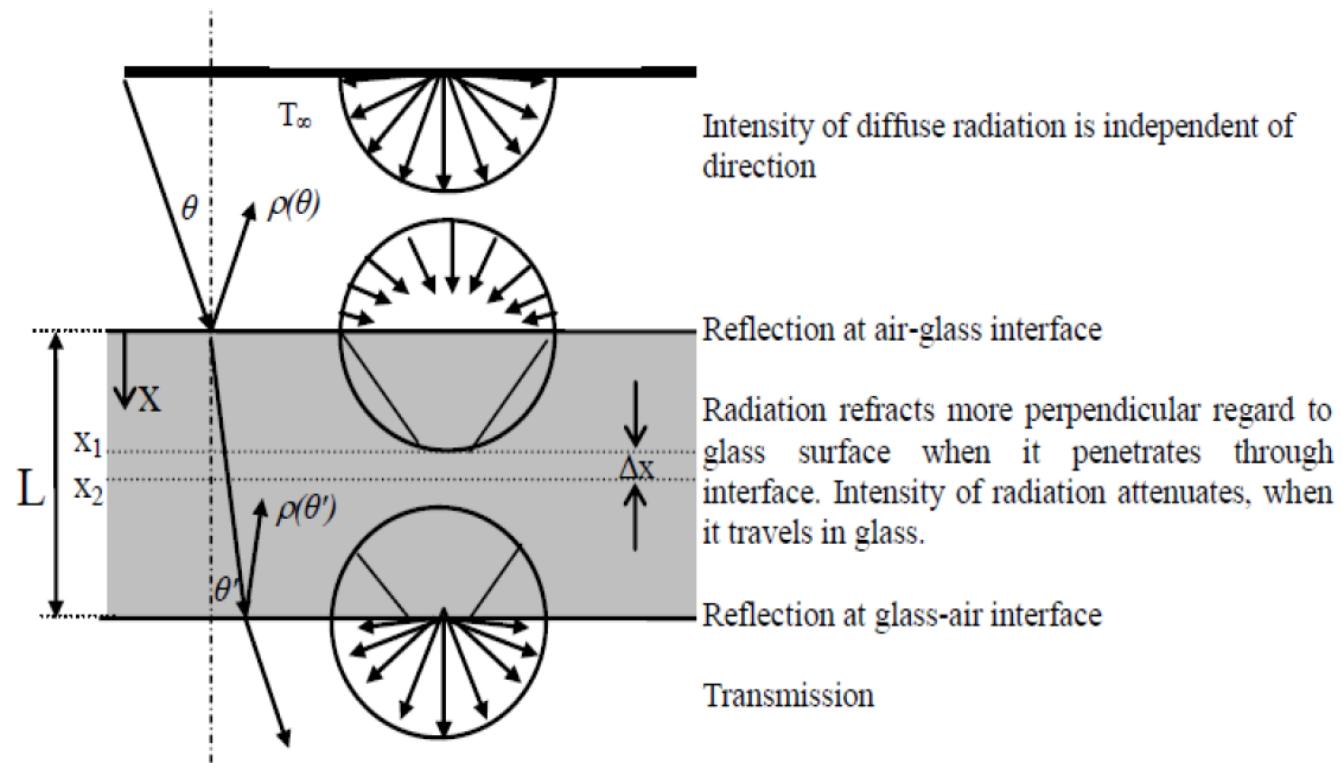
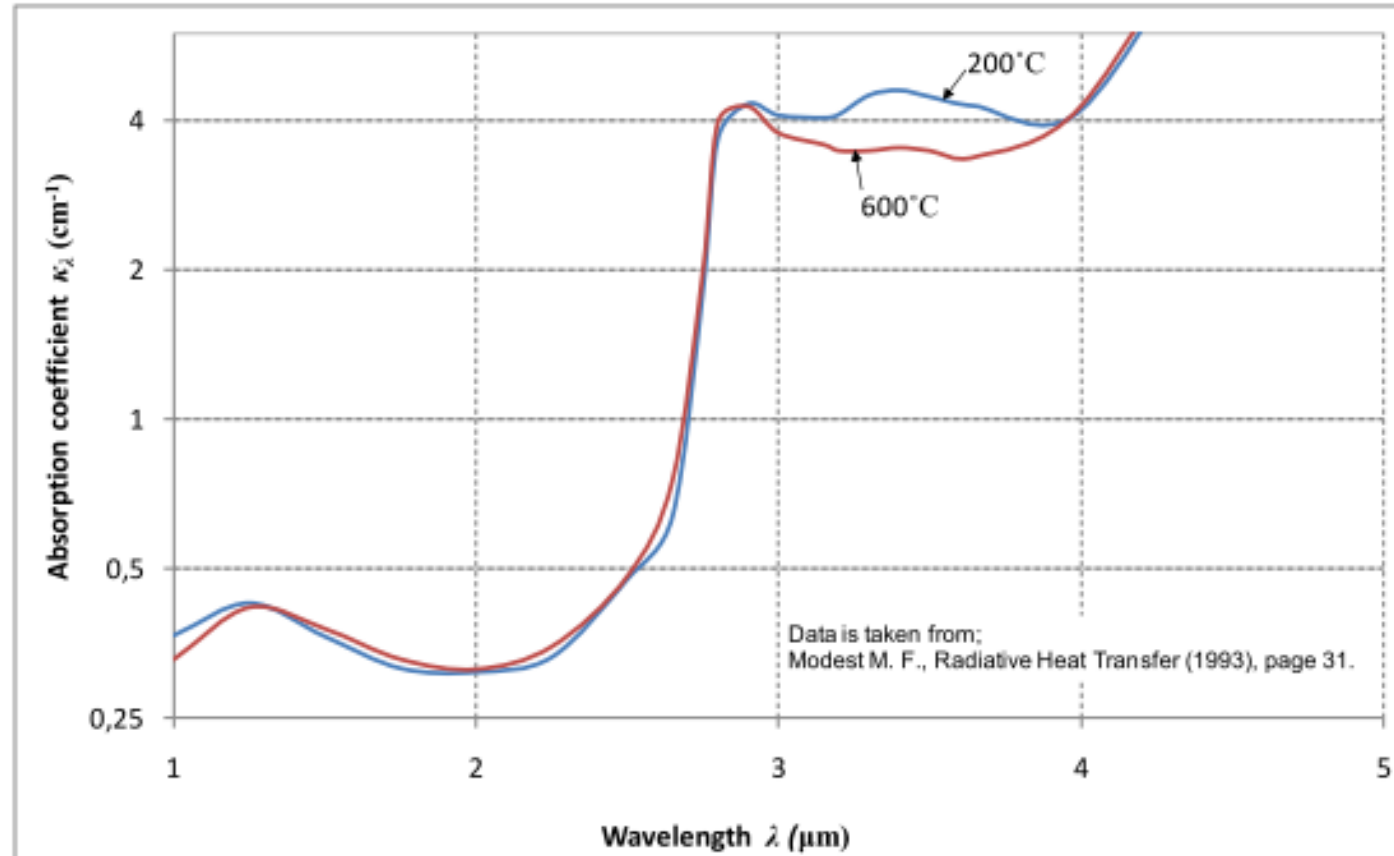


Figure 7.2. Hemispherical spectral emissive power of blackbody at various blackbody temperatures

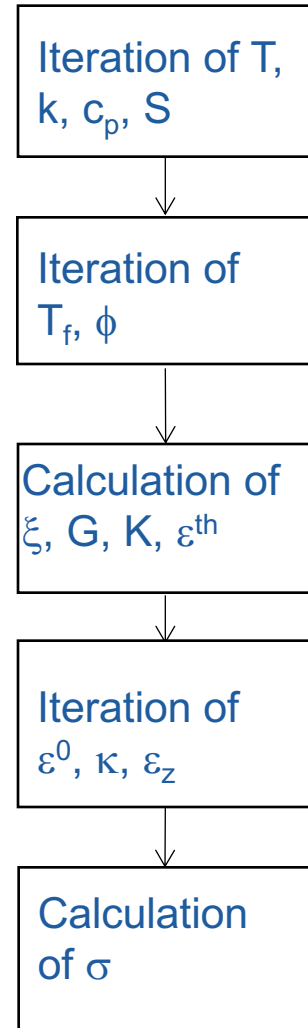
Behavior of incident radiation



Absorption coefficient in glass



$$i_x = i_0 e^{-\kappa x}$$



$$\rho c_{pg}(T) \frac{\partial T}{\partial t} = \frac{\partial}{\partial x} \left(k(T) \frac{\partial T}{\partial x} \right) + S(T, x)$$

$$S(T, x) \approx \sum_{i=1, j=2}^{i=k, j=k+1} \left\{ \left[F_b(\lambda_i, \lambda_j, T_\infty) \sigma T_\infty^4 - F_b(\lambda_i, \lambda_j, T_\infty) \sigma T^4 \right] \cdot \frac{(1 - \rho_m)}{1 - \rho_m e^{-a(\Delta\lambda_i)L/\cos\alpha_m}} \cdot \left[e^{-a(\Delta\lambda_i)x_1/\cos\alpha_m} - e^{-a(\Delta\lambda_i)x_2/\cos\alpha_m} + e^{-a(\Delta\lambda_i)(L-x_1)/\cos\alpha_m} - e^{-a(\Delta\lambda_i)(L-x_2)/\cos\alpha_m} \right] \right\}$$

$$\phi(t) = \exp \left(\frac{H}{R} \left(\frac{1}{T_{ref}} - \frac{x}{T(t)} - \frac{1-x}{T_f(t)} \right) \right) \quad T_{fi}(t) = \frac{\lambda_i T_{fi}(t - \Delta t) + \Delta t T(t) \phi(t)}{\lambda_i + \Delta t \phi(t)} \quad T_f(t) = \sum_{i=1}^n C_i T_{fi}(t)$$

$$\Delta \varepsilon^{th}(t) = (\alpha_l - \alpha_g)(T_f(t) - T_f(t - \Delta t)) + \alpha_g(T(t) - T(t - \Delta t))$$

$$\xi(t) = \int_0^t \phi(t') dt' \quad G(\xi(t)) = G_\infty + (G_0 - G_\infty) \sum_{i=1}^n w_{1i} \exp \left(-\frac{\xi(t)}{\tau_{1i}} \right) \quad K(\xi(t)) = K_\infty + (K_0 - K_\infty) \sum_{i=1}^n w_{2i} \exp \left(-\frac{\xi(t)}{\tau_{2i}} \right)$$

$$\sigma_{ij}(t) = \delta_{ij} \int_0^t K(\xi(t) - \xi(t')) \frac{d(\varepsilon_{kk}(t') - 3\varepsilon^{th}(t'))}{dt'} dt' + 2 \int_0^t G(\xi(t) - \xi(t')) \frac{d \left(\varepsilon_{ij}(t') - \frac{\delta_{ij} \varepsilon_{kk}(t')}{3} \right)}{dt'} dt'$$

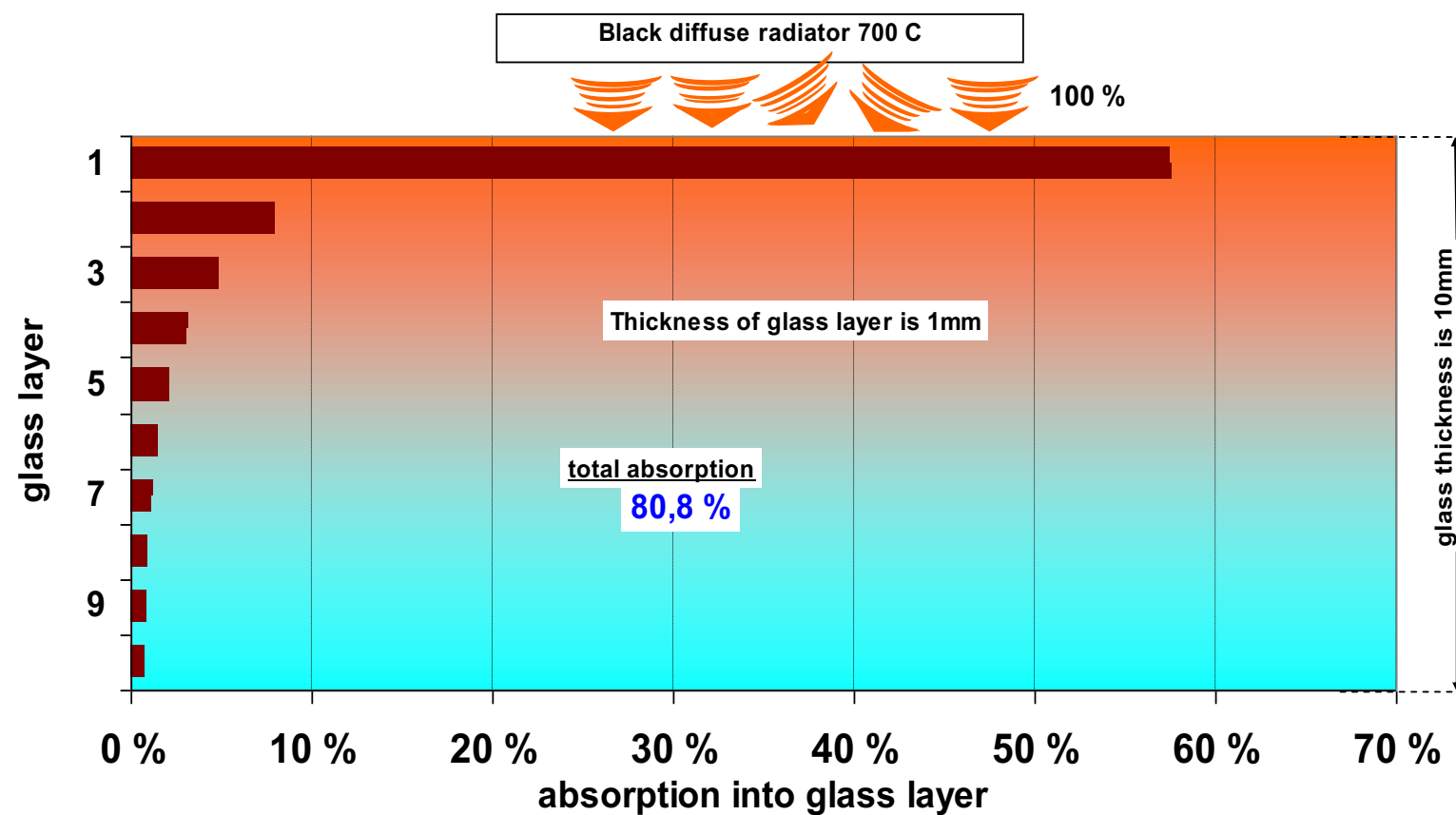
$$\int_{-b/2}^{b/2} \sigma(z, t) dz = N$$

$$\int_{-b/2}^{b/2} \sigma(z, t) z dz = M$$

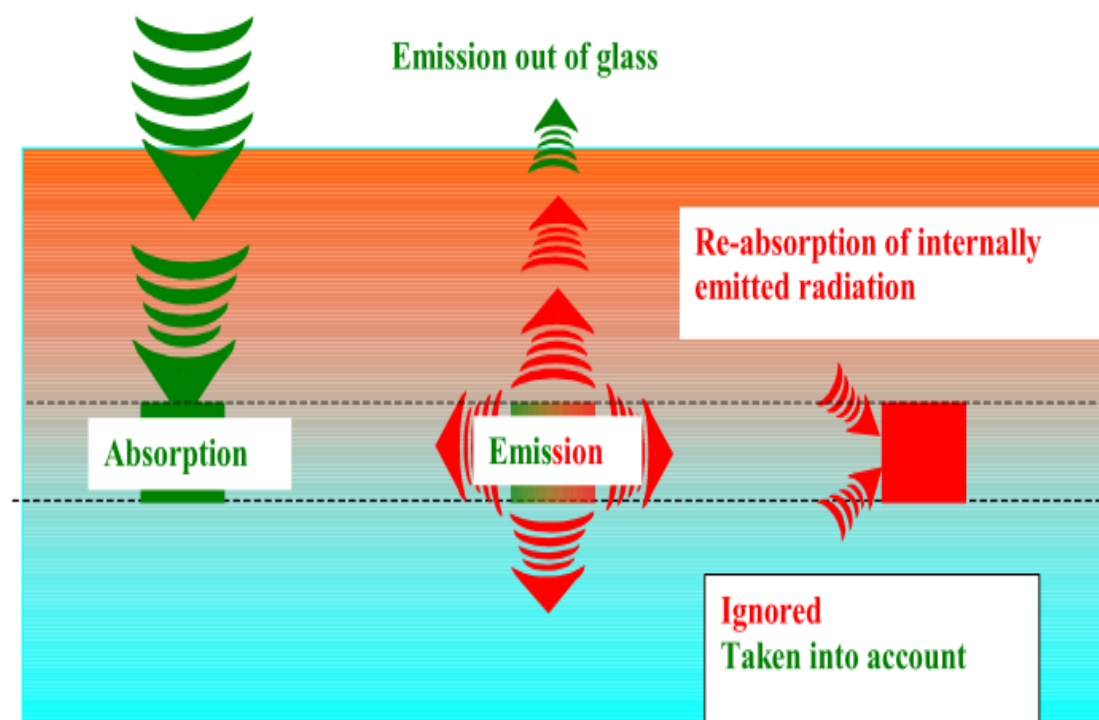
$$\varepsilon_x = \varepsilon_y = \varepsilon^0 + \kappa z$$

Plane stress $\sigma_z = 0$

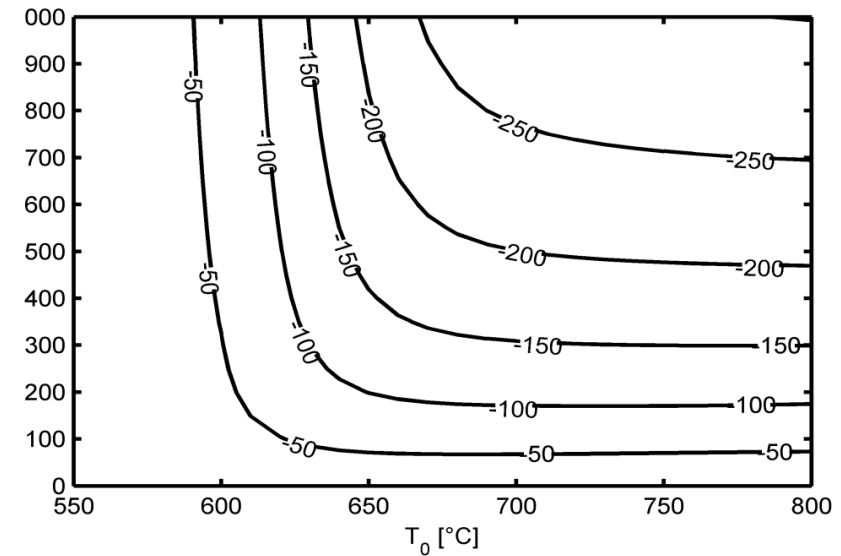
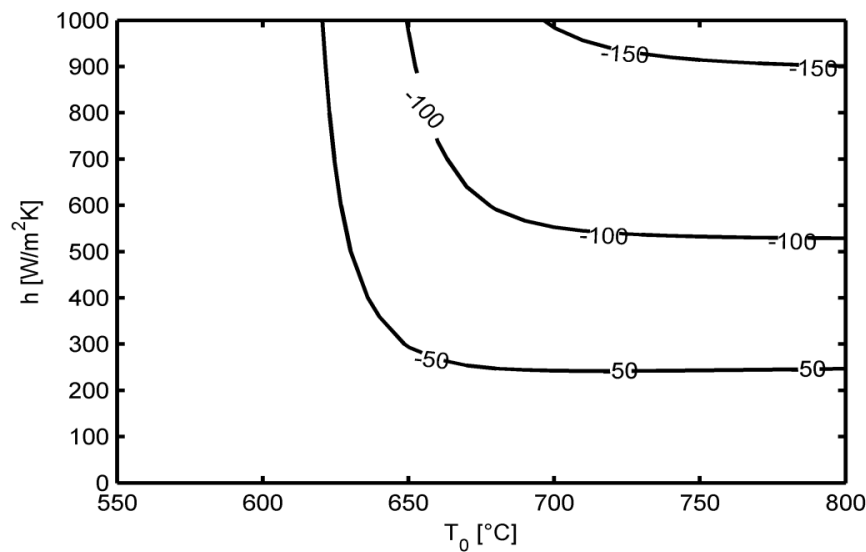
Absorption of radiation



Simplified treatment of radiation in glass



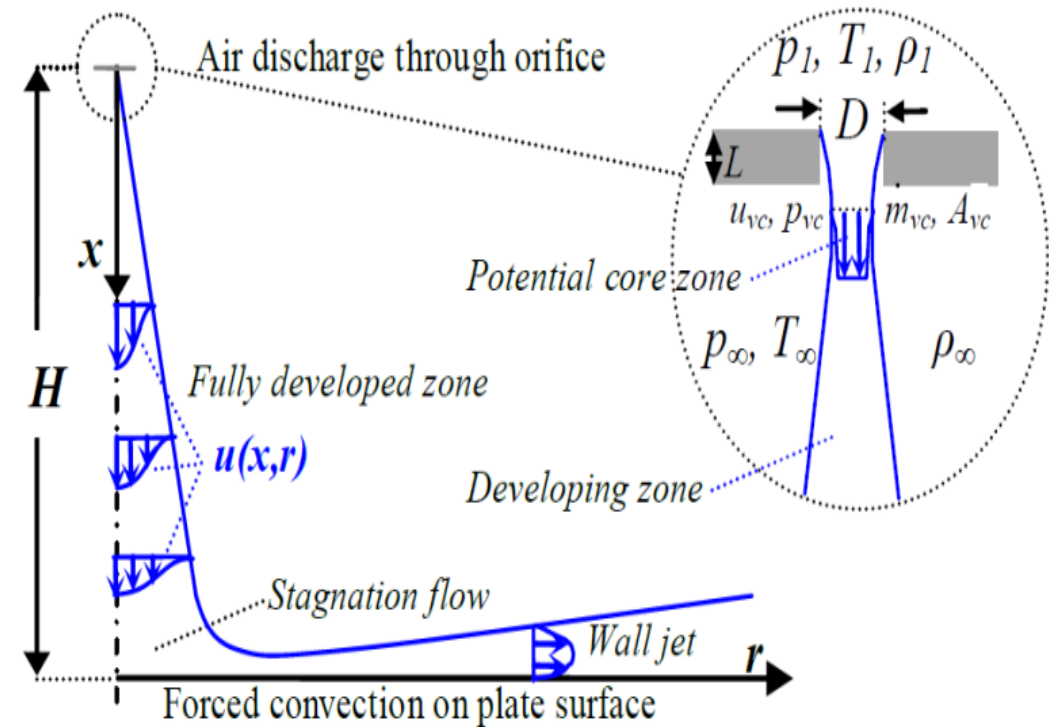
Surface residual stress



Required heat transfer coefficient vs. initial glass temperature. Parameters: glass thickness (2 mm left, 6 mm right) and compression surface stress (MPa)

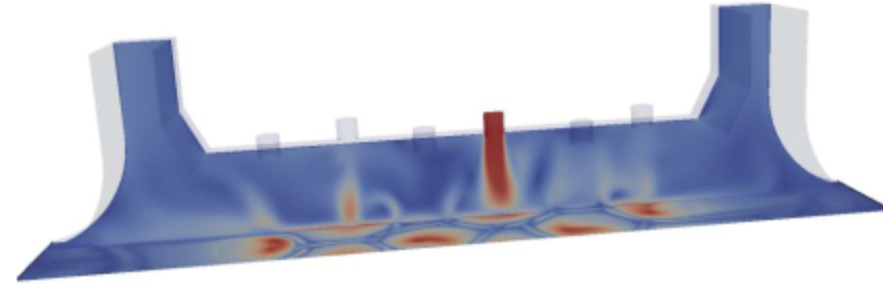
Impinging jet heat transfer

- Existing correlations are functions of Re , r/d , H/d , and Pr
- Measurements and CFD simulations show that temperature affects the results
- Mach number also affects the heat transfer
- Correlations are superior to CFD in design optimization because of their speed and reliability



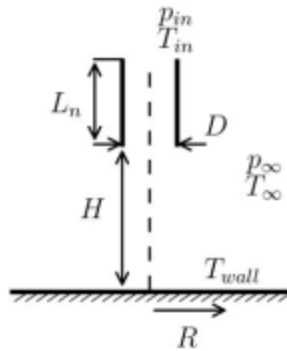
Modelling

Impinging Jet
Heat Transfer



Correlations

$$\frac{\overline{Nu}}{Pr^{0.42}} = \frac{D}{R} \frac{1 - 1.1 \left(\frac{D}{R}\right)}{1 + 0.1 \left(\frac{H}{D} - 6\right) \frac{D}{R}} 2Re^{\frac{1}{2}} \left(1 + \frac{Re^{0.55}}{200}\right)^{\frac{1}{2}}$$



Finite Volume
Method

LES, DNS, etc.

Compressible

$$\frac{\partial(\rho u_j)}{\partial x_j} = 0$$

Incompressible

$$\frac{\partial(u_j)}{\partial x_j} = 0$$

RANS

$$-\rho u_i u_j = 2\mu_t \left[S_{ij} - \frac{1}{3} S_{kk} \delta_{ij} \right]$$

k - ω - SST

$$\mu_t = \frac{a_1 \rho k}{\max(a_1 \omega_1 S F_2)}$$

$P = ?$

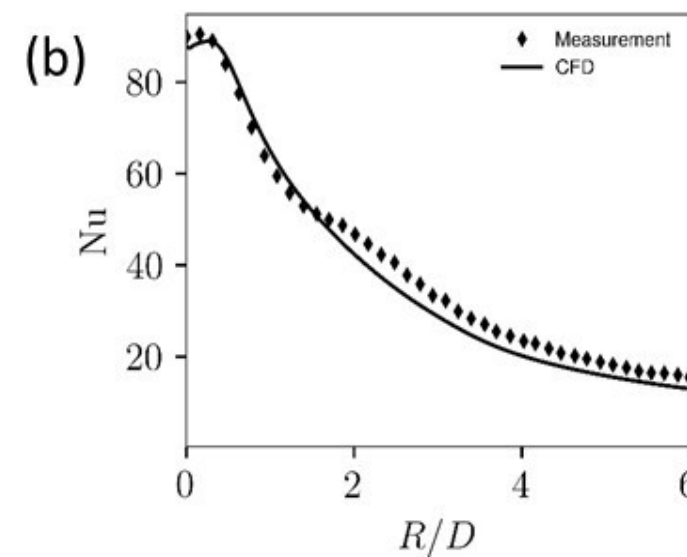
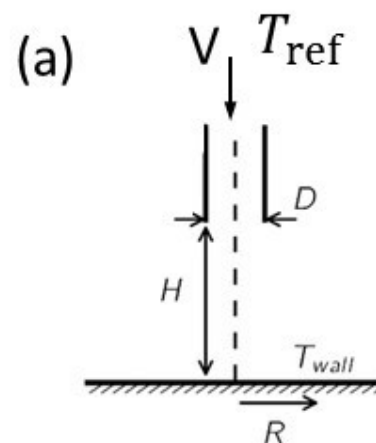
Modeling of jet convection with OpenFOAM

$$\frac{\partial(\rho k)}{\partial t} + \frac{\partial(\rho U_j k)}{\partial x_j} = \tilde{P}_k - \beta^* \rho k \omega + \frac{\partial}{\partial x_i} \left[(\mu + \sigma_k \mu_t) \frac{\partial k}{\partial x_i} \right]$$

$$\begin{aligned} \frac{\partial(\rho \omega)}{\partial t} + \frac{\partial(\rho U_i \omega)}{\partial x_i} &= \frac{\alpha \tilde{P}_k}{\nu_t} - \beta \rho \omega^2 + \frac{\partial}{\partial x_i} \left[(\mu + \sigma_\omega \mu) \frac{\partial \omega}{\partial x_i} \right] \\ &+ 2(1 - F_1) \rho \sigma_\omega^2 \frac{1}{\omega} \frac{\partial k}{\partial x_i} \frac{\partial \omega}{\partial x_i} \end{aligned} \quad (3)$$

$$\tilde{P} = \min(P, 10\beta^* \rho \omega k)$$

$$P = \text{grad}(U) : (2\mu_t \text{dev}(S) - \frac{2}{3} \rho k I)$$



Turbulence

k – ω – SST

$$\begin{aligned}
 \frac{\partial(\rho k)}{\partial t} + \frac{\partial(\rho U_j k)}{\partial x_j} &= \tilde{P} - \beta^* \rho k \omega \\
 &+ \frac{\partial}{\partial x_i} \left[(\mu + \sigma_k \mu_t) \frac{\partial k}{\partial x_i} \right] \\
 \frac{\partial(\rho \omega)}{\partial t} + \frac{\partial(\rho U_j \omega)}{\partial x_j} &= \frac{\alpha \tilde{P}}{\nu_t} - \beta \rho \omega^2 \\
 &+ \frac{\partial}{\partial x_i} \left[(\mu + \sigma_\omega \mu_t) \frac{\partial \omega}{\partial x_i} \right] \\
 &+ 2(1 - F_1) \rho \sigma_{\omega 2} \frac{1}{\omega} \frac{\partial k}{\partial x_i} \frac{\partial \omega}{\partial x_i}
 \end{aligned}$$

Production Terms

- Menter 2003

$$\tilde{P} = \min(P, 10\beta^* \rho \omega k)$$

$$P = \mu_t \frac{\partial U_i}{\partial x_j} \left[\frac{\partial U_i}{\partial x_j} + \frac{\partial U_j}{\partial x_i} \right]$$

- OpenFOAM 3.0.1

$$P = \mu_t \frac{\partial U_i}{\partial x_j} \left(\text{dev} \left(\left[\frac{\partial U_i}{\partial x_j} + \frac{\partial U_j}{\partial x_i} \right] \right) - \frac{2}{3} \rho k \sigma_{ij} \right)$$

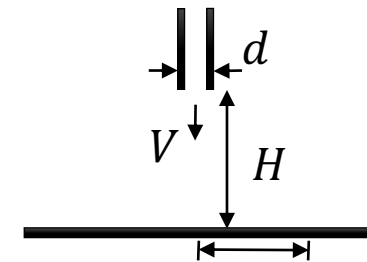
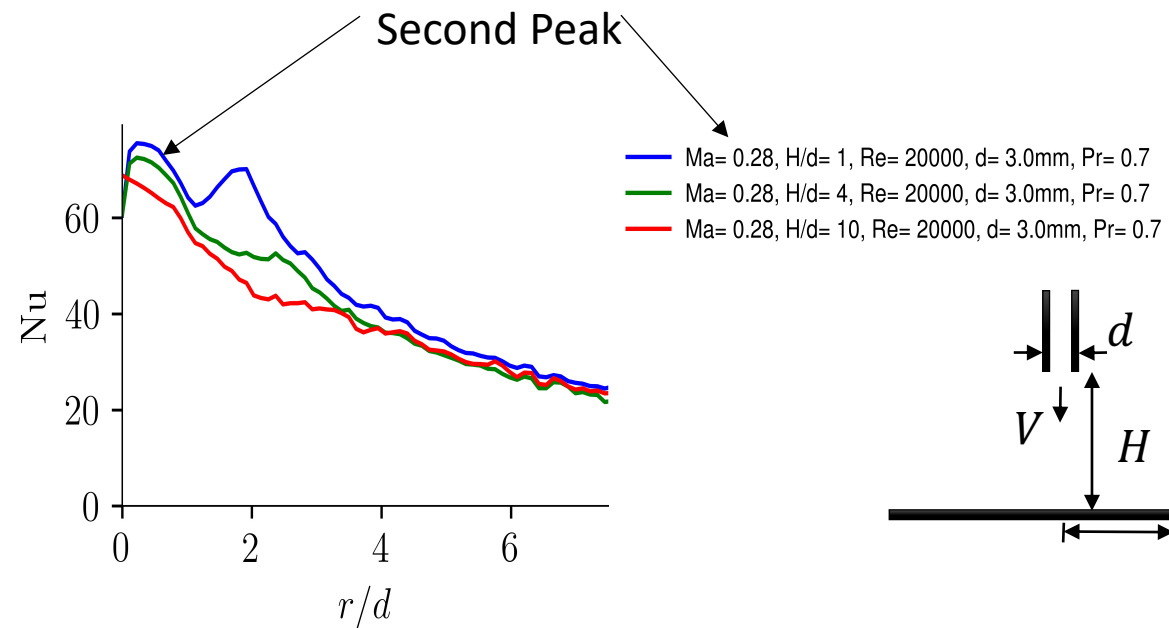
- Vorticity Based

$$P = \mu_t \Omega^2 - \frac{2}{3} \rho k \delta_{ij} \frac{\partial u_i}{\partial x_j}$$

$$\Omega = \sqrt{2W_{ij}W_{ij}}, W_{ij} = \frac{1}{2} \left(\frac{\partial U_i}{\partial x_j} - \frac{\partial U_j}{\partial x_i} \right)$$

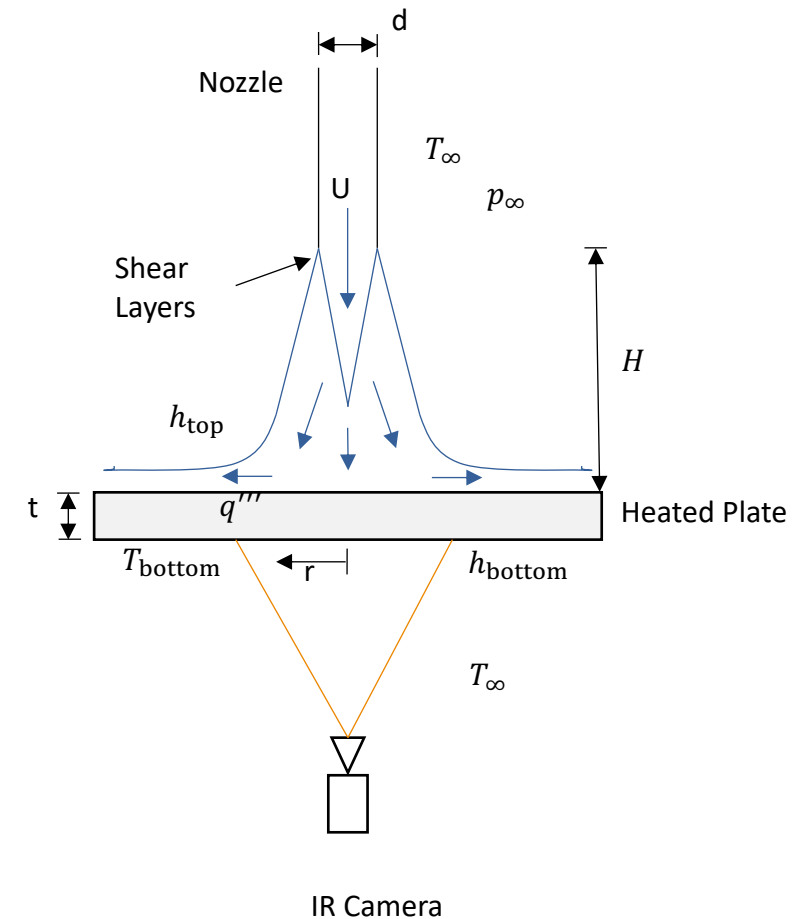
Effect of nozzle distance vs. diameter, H/d

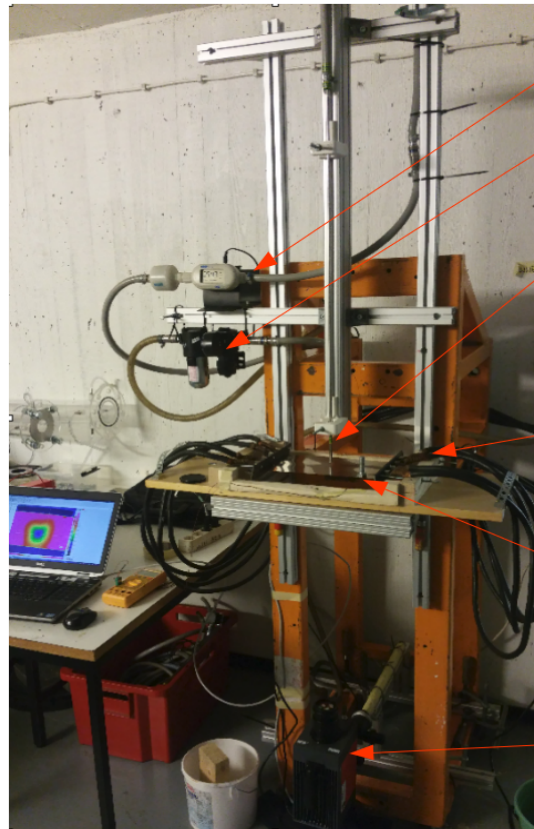
- The closer the nozzle the better heat transfer, usually.
- The closer the nozzle the more difficult to model
- The closer the nozzle the more non-uniform heat transfer



Measurements

- Existing correlations do not take into account the wall temperature or Mach number
- Measurement of local heat transfer by IR camera and inverse analysis to calculate heat transfer coefficient





Mass flow meter

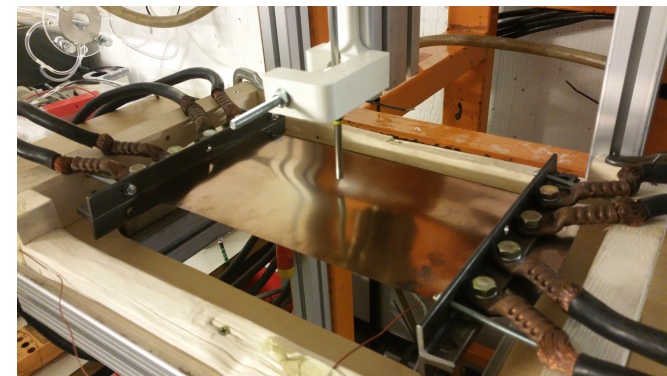
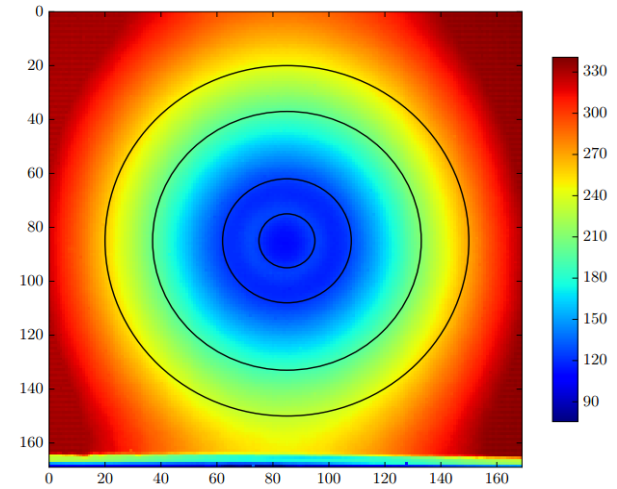
Pressure regulator

Nozzle

DC supply (100-1000A)

Heated metal plate (0.2mm)

IR camera

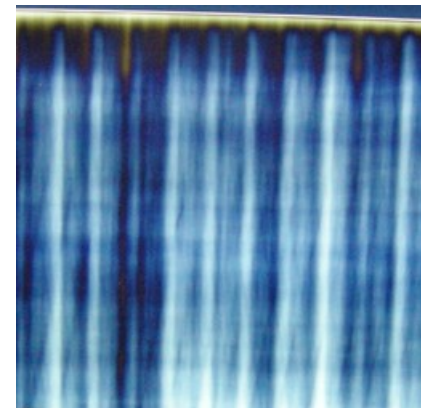
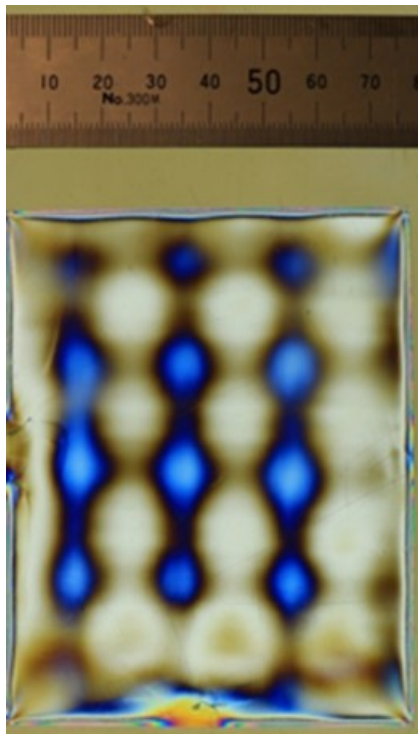


#GPD2017

GLASS PERFORMANCE DAYS 2017

1 2 3 4 5 6 7 8 9 10 11 12 13 14 15 16 17 18 19 20 21 22 23 24 25

GB
25
YEARS



Stresses and strains

Iteration of T ,
 k , c_p

$$\rho c_{pg}(T) \frac{\partial T}{\partial t} = \frac{\partial}{\partial x} \left(k(T) \frac{\partial T}{\partial x} \right)$$

Iteration of
 T_f , ϕ

$$\phi(t) = \exp \left(\frac{H}{R} \left(\frac{1}{T_{ref}} - \frac{x}{T(t)} - \frac{1-x}{T_f(t)} \right) \right) \quad T_{fi}(t) = \frac{\lambda_i T_{fi}(t - \Delta t) + \Delta t T(t) \phi(t)}{\lambda_i + \Delta t \phi(t)} \quad T_f(t) = \sum_{i=1}^n C_i T_{fi}(t)$$

Calculation of
 ξ , G , K , ε^{th}

$$\Delta \varepsilon^{th}(t) = (\alpha_l - \alpha_g)(T_f(t) - T_f(t - \Delta t)) + \alpha_g(T(t) - T(t - \Delta t))$$

$$\xi(t) = \int_0^t \phi(t') dt' \quad G(\xi(t)) = G_\infty + (G_0 - G_\infty) \sum_{i=1}^n w_{1i} \exp \left(-\frac{\xi(t)}{\tau_{1i}} \right) \quad K(\xi(t)) = K_\infty + (K_0 - K_\infty) \sum_{i=1}^n w_{2i} \exp \left(-\frac{\xi(t)}{\tau_{2i}} \right)$$

Iteration of
 ε^0 , κ , ε_z

$$\sigma_{ij}(t) = \delta_{ij} \int_0^t K(\xi(t) - \xi(t')) \frac{d(\varepsilon_{kk}(t') - 3\varepsilon^{th}(t'))}{dt'} dt' + 2 \int_0^t G(\xi(t) - \xi(t')) \frac{d\left(\varepsilon_{ij}(t') - \frac{\delta_{ij} \varepsilon_{kk}(t')}{3} \right)}{dt'} dt'$$

$$\int_{-b/2}^{b/2} \sigma(z, t) dz = N$$

$$\int_{-b/2}^{b/2} \sigma(z, t) z dz = M$$

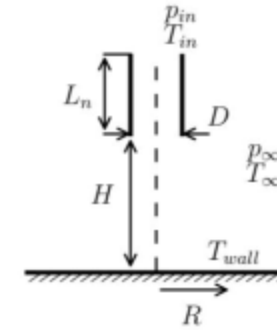
Calculation
of σ

$$\varepsilon_x = \varepsilon_y = \varepsilon^0 + \kappa z$$

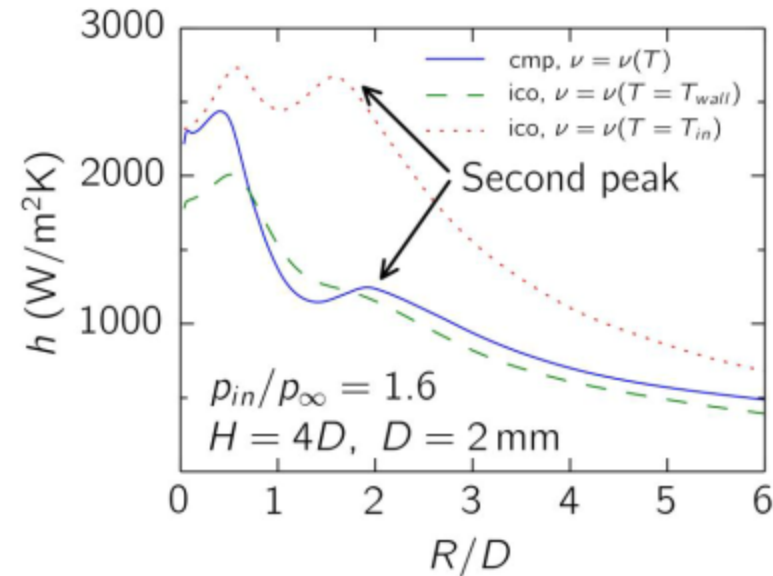
Plane
stress

$$\sigma_z = 0$$

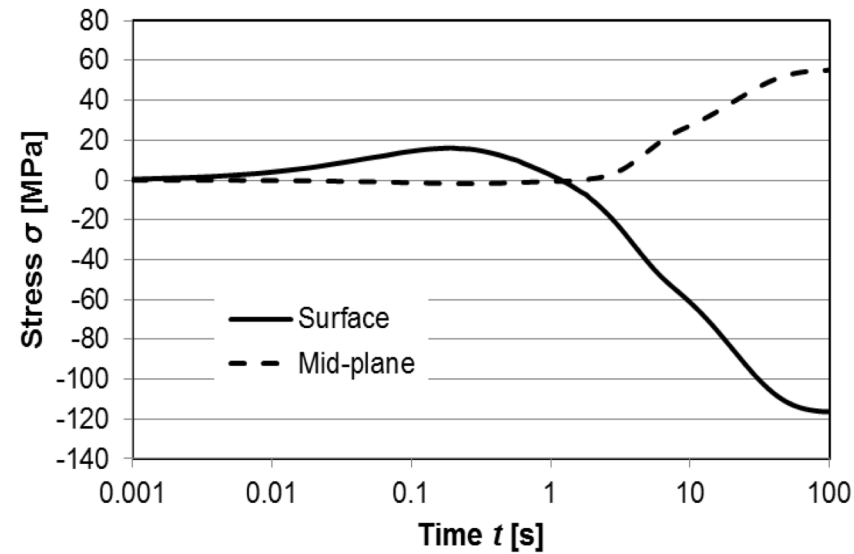
Fluid Properties



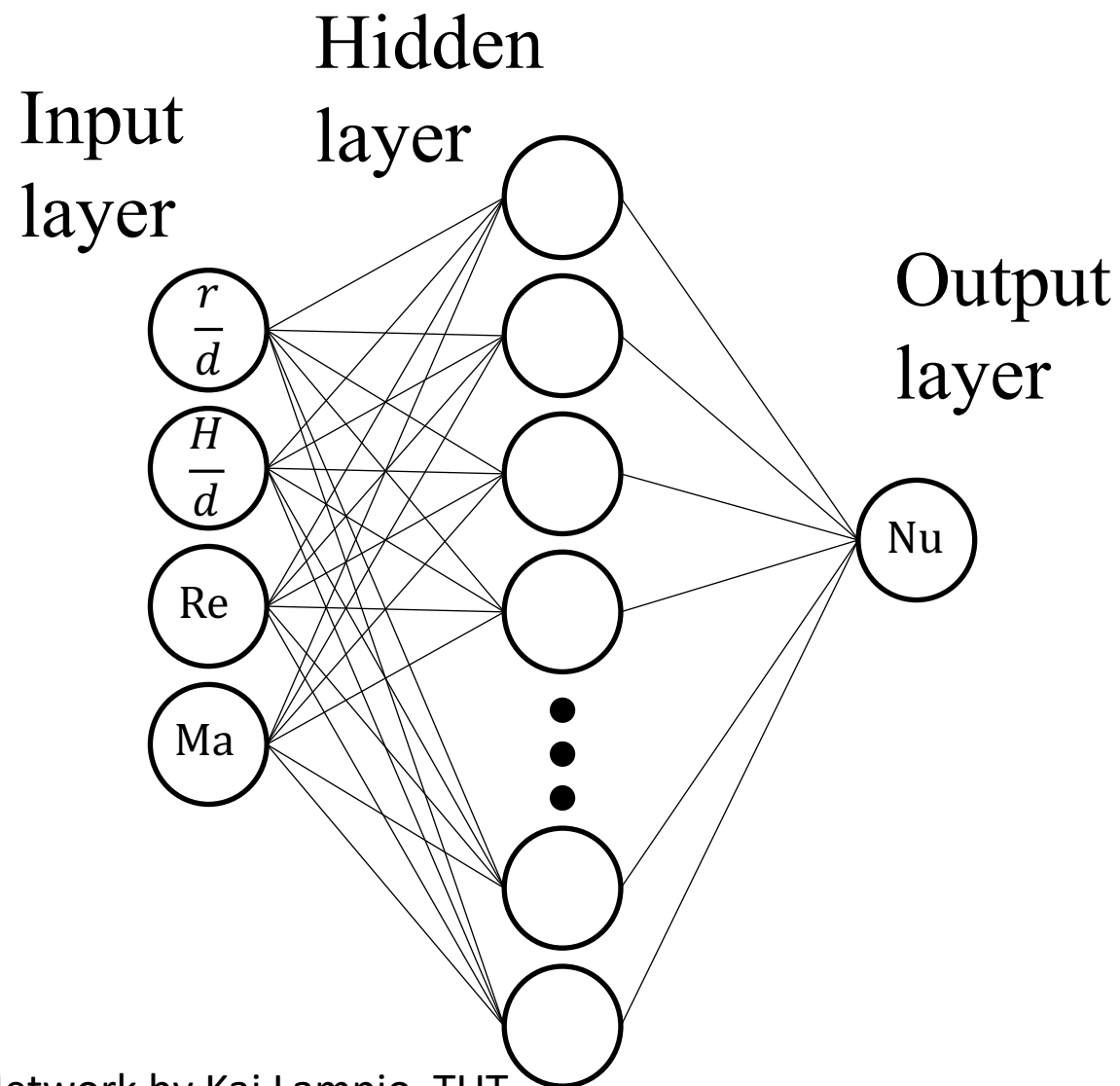
- Compressible Flow
 - Sutherland, $\nu = \nu(T)$
 - Ideal Gas, $\rho = \rho(p, T)$
- Incompressible
 - Given ρ and ν
 - $\nu(T = 20^\circ\text{C}) \approx 1.5 \times 10^{-5} \text{ m}^2/\text{s}$
 - $\nu(T = 600^\circ\text{C}) \approx 9.6 \times 10^{-5} \text{ m}^2/\text{s}$



Residual stress development during cooling

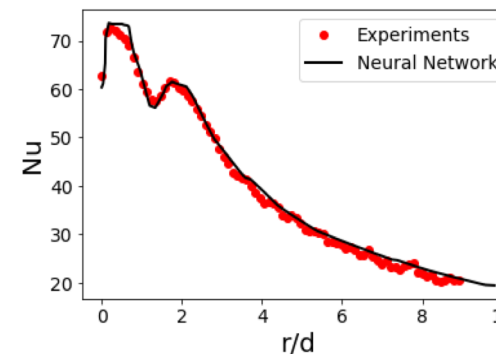


Time-dependent stress on the surface and mid-plane during the cooling.

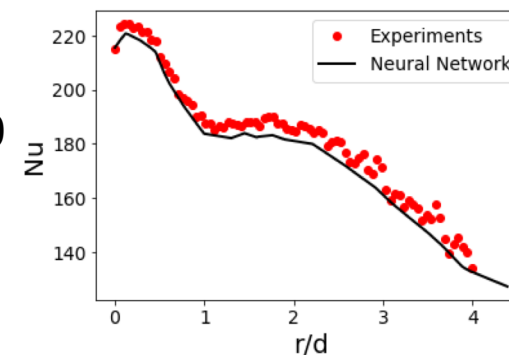


Neural Network by Kaj Lampio, TUT

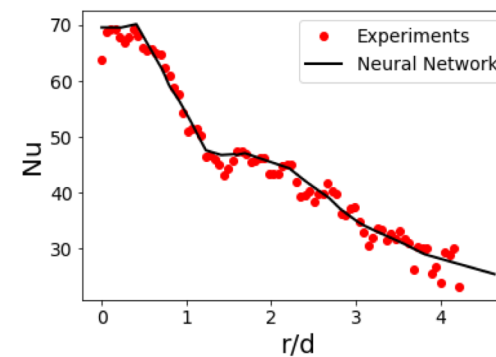
$Re = 20100$
 $Ma = 0.30$
 $H/d = 2$



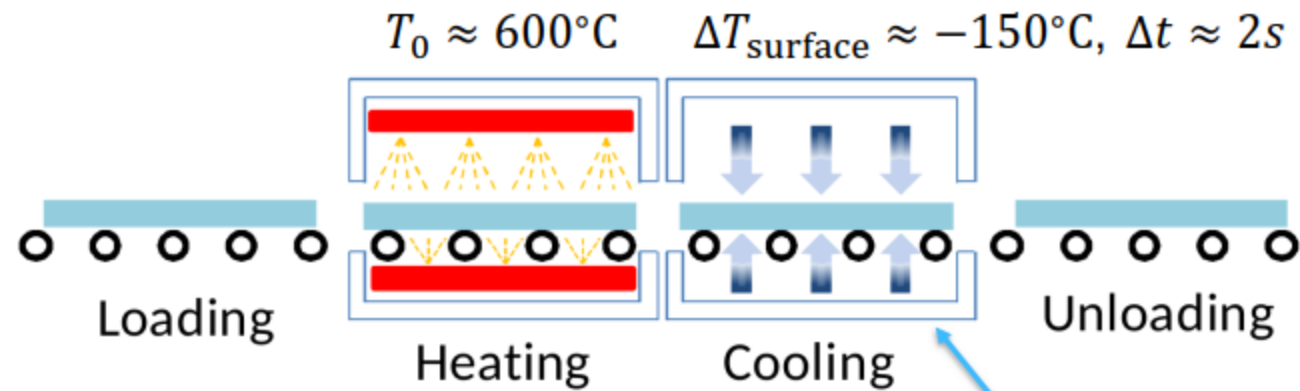
$Re = 94300$
 $Ma = 0.71$
 $H/d = 4$



$Re = 10100$
 $Ma = 0.075$
 $H/d = 3$



Thin Glass Tempering



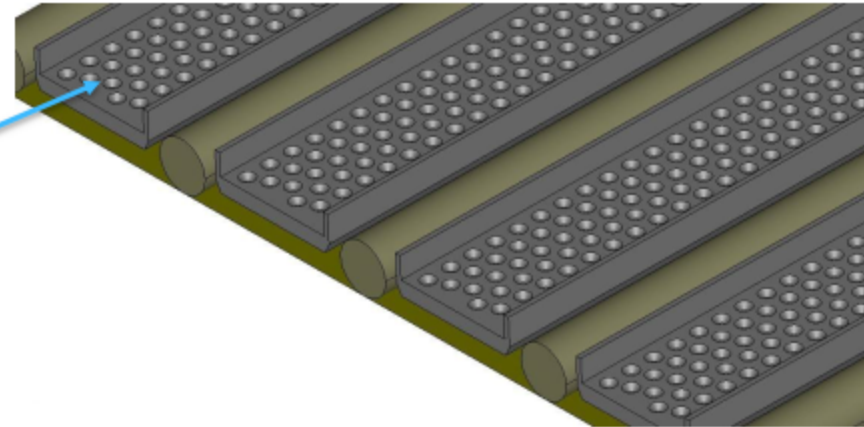
Aronen 2012 [1]

Cooling Jets

$\text{Ma} \approx 0.85$

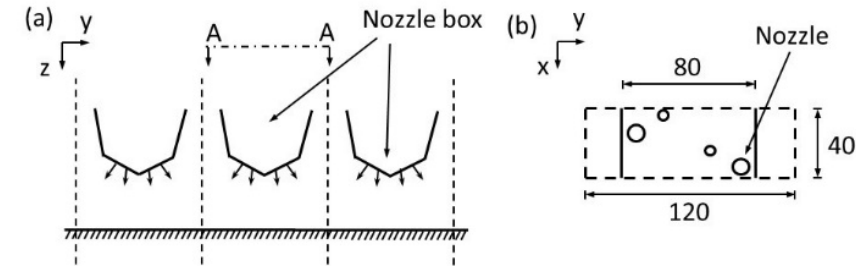
$d_{\text{nozzle}} \approx 1 - 3 \text{ mm}$

$\bar{h} \approx 1000 \text{ W/m}^2\text{K}$

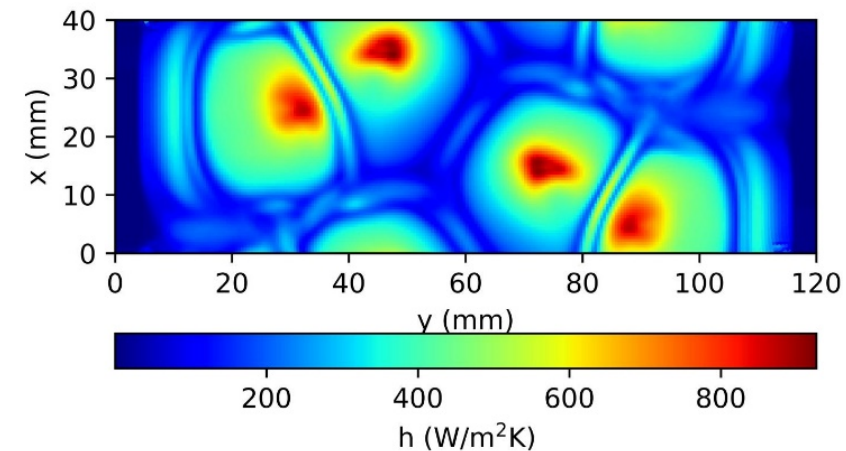


Cooling heat transfer in tempering process

- Wall heat transfer coefficient is calculated using CFD
- The calculation is done for one periodic part of a quenching machine
- Takes about 6h with 12 cores
- Estimated time to model the whole geometry is $1200 \times 6h = 300d$



Schematic of the nozzles (a) and locations in nozzle plate (b).



Distribution of heat transfer coefficient

Effect of nozzle locations on heat transfer

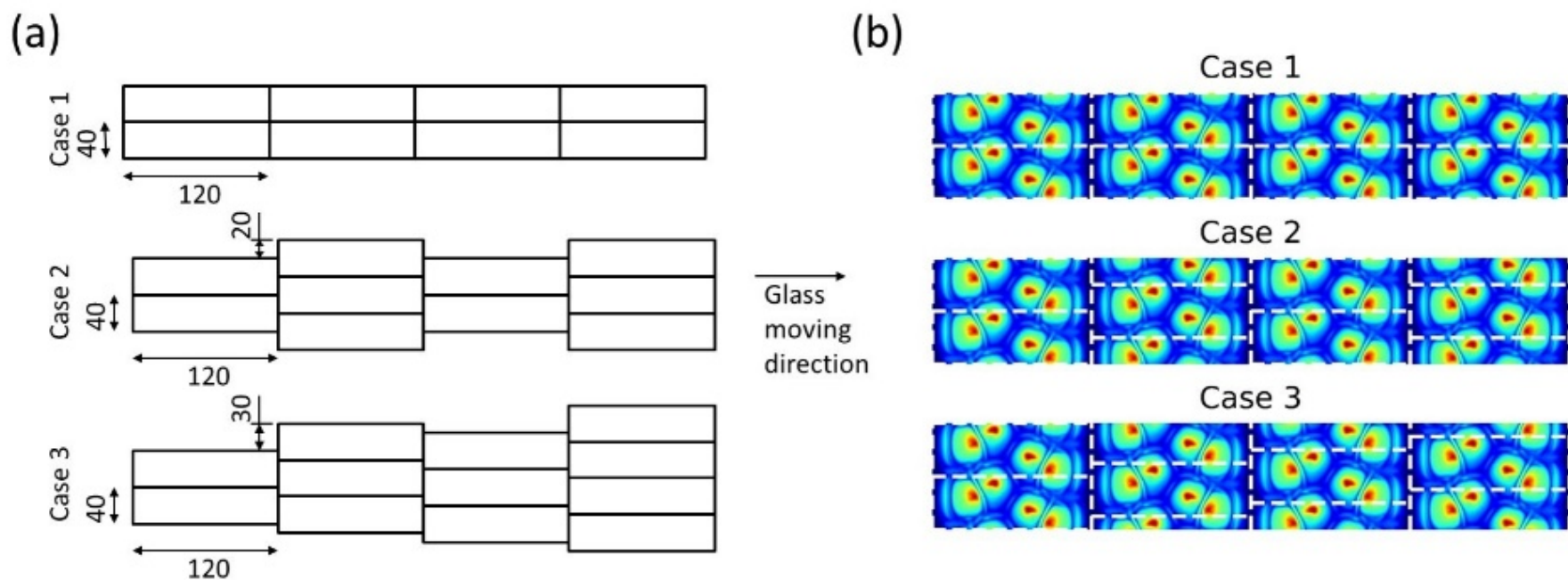
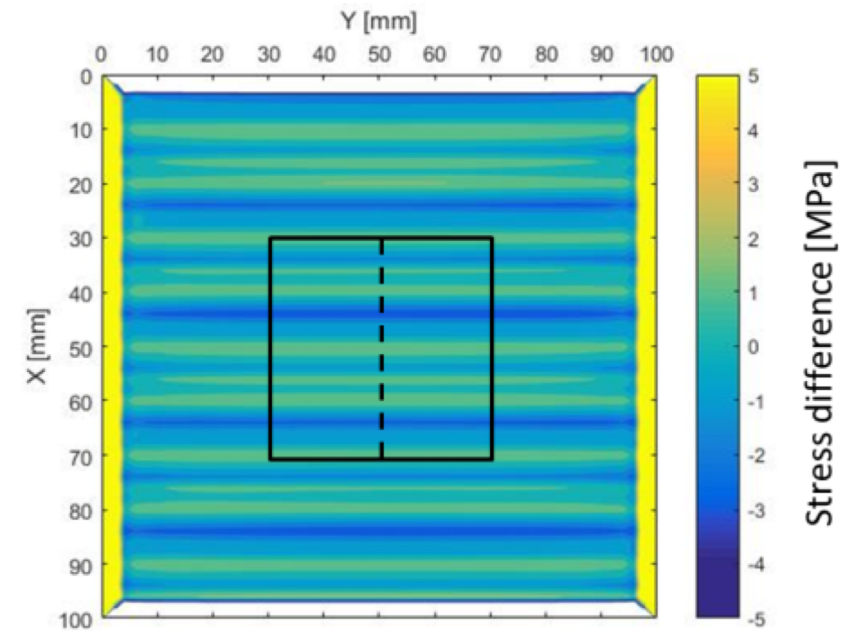


Illustration of periodic locations of nozzles and heat transfer coefficients. (a) Schematics. (b) Heat transfer coefficients. Dimensions are in mm.

Residual stresses

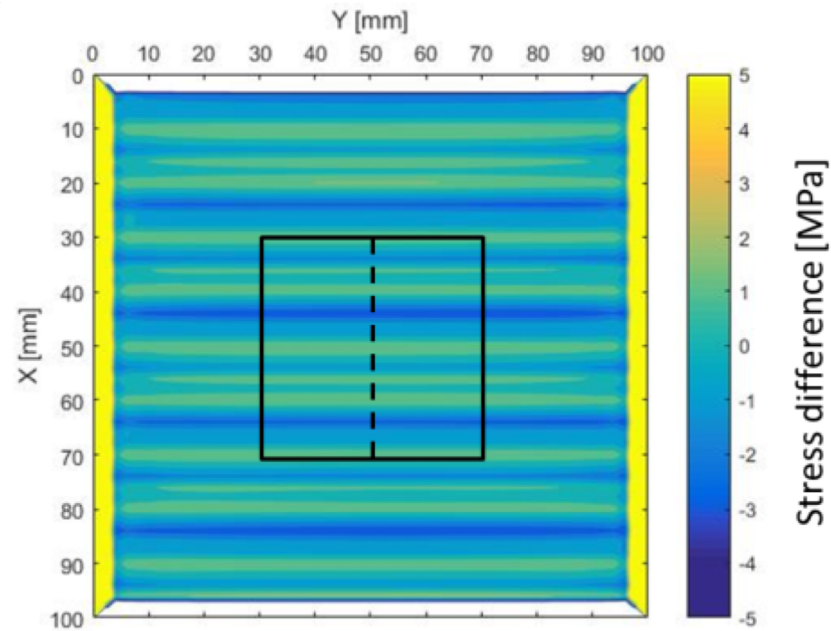
- Using calculated heat transfer coefficients a separated residual stress simulation is made
- Results of Case 1 is shown on the right



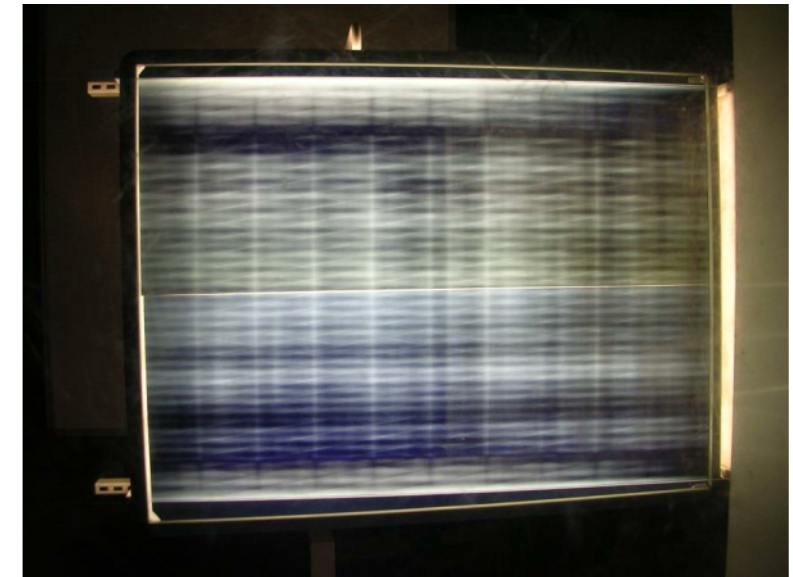
Stress difference $\sigma_x - \sigma_y$ at the surface

Connection between residual stress and anisotropy

- Similar horizontal stripes
- Other defects also visible

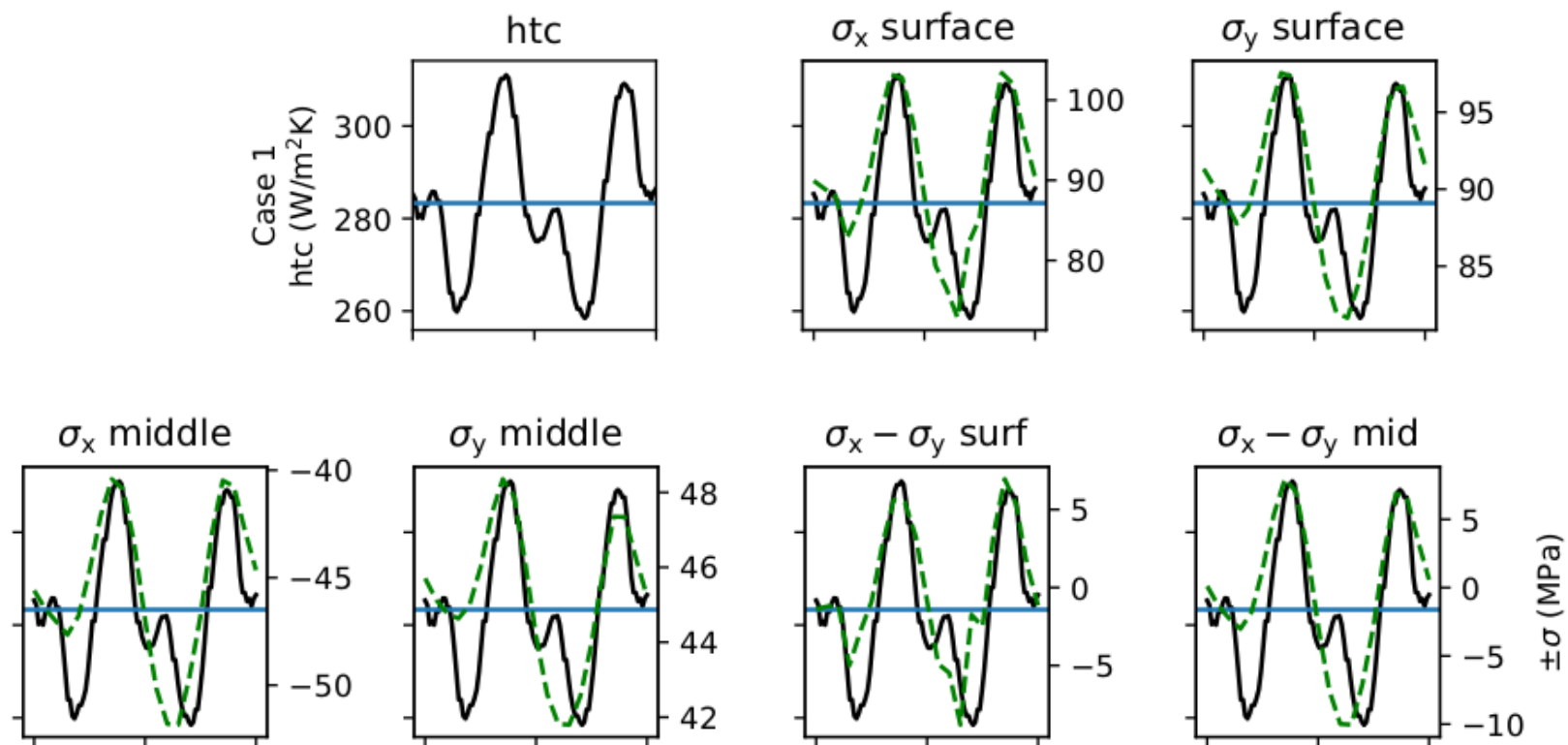


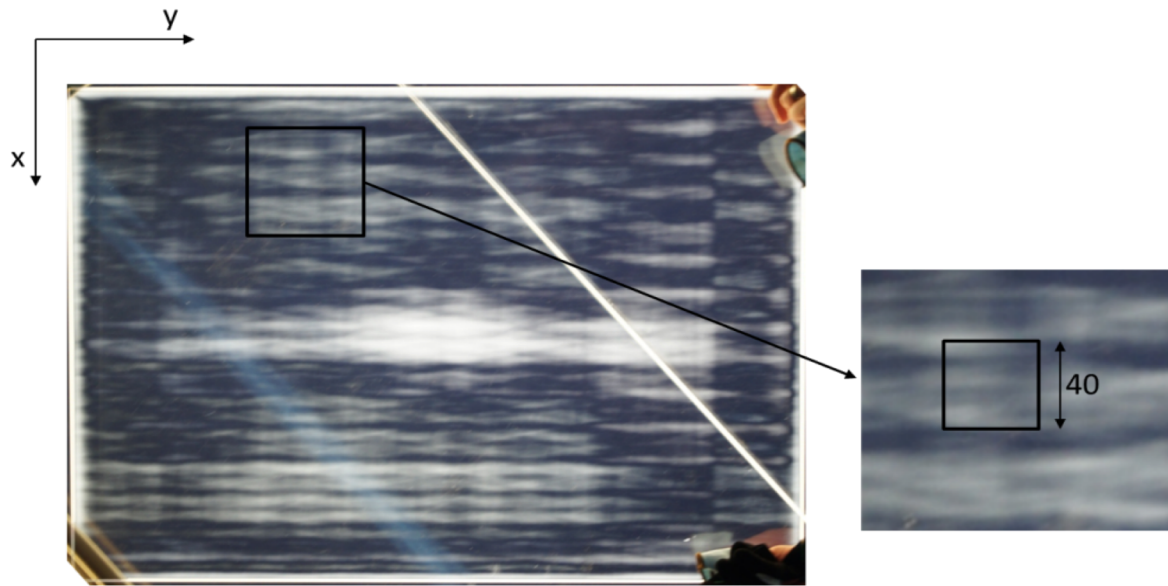
Stress difference $\sigma_x - \sigma_y$ at the surface



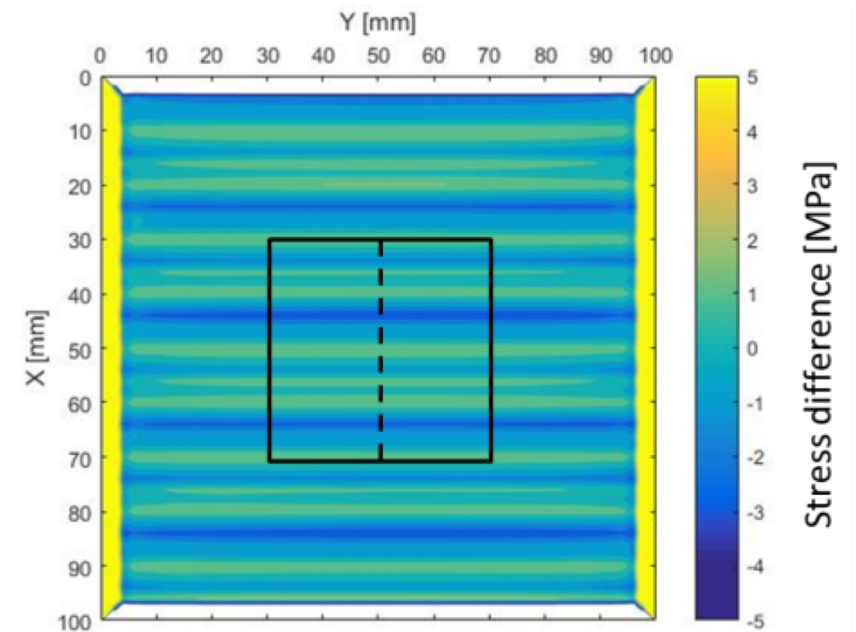
Typical stress pattern of flat tempered glass seen through polarized filters

Heat transfer coefficients and residual stresses





The anisotropy distribution of 585x800 mm tempered glass plate. In the enlarged area on the right the 40x40 mm is marked to present the similar area



Conclusions

- Residual stresses and anisotropy are related each other
- Numerical values between variations of residual stress and heat transfer coefficient are similar
- Visual observations with polarized light give similar patterns as calculated residual stress

The authors acknowledge the Finnish Funding Agency for Technology and Innovation (Tekes) for partly funding this work during the program Energy Efficient Tempering of Thin Glasses for Solar Energy Next Generation Products. The authors also acknowledge the University of Sydney HPC service at The University of Sydney for providing HPC and software resources that have contributed to the research results reported within this paper.

